Chapter 11

Effects of Solar Radio Bursts on Wireless Systems

Dale E. Gary[1], Louis J. Lanzerotti[1,2], Gelu M. Nita[1], David J. Thomson[3]
1. *Center for Solar-Terrestrial Research, New Jersey Institute of Technology Newark, NJ 07102, USA*
2. *Bell Laboratories, Lucent Technologies, Murray Hill, NJ 07974 USA*
3. *Queens University, Kingston, Ontario K7L 3N6, Canada*

Abstract We review the state of current understanding of the potential for interference and interruption of service of wireless communications systems due to solar radio bursts. There have been several reported instances of an enhanced rate of dropped cell-phone calls during solar bursts, and the design of current base station systems make them vulnerable to problems near sunrise and sunset for antennas facing in the direction of the Sun during outbursts. It is likely that many cases of interference have gone unreported and perhaps unrecognized. We determine the level of radio noise that can cause potential problems, and then discuss how often bursts of the required magnitude might happen. We illustrate the range of radio flux behavior that may occur, in both frequency and time, with data from the Solar Radio Spectropolarimeter and the Owens Valley Solar Array. We find that bursts that can cause potential problems occur on average once every 3.5 days at solar maximum, but also occur at a reduced rate of 18.5 days between events at solar minimum. We investigate the rate of occurrence as a function of frequency, which is relevant for future wireless systems that will operate at higher frequencies than the present systems.

Keywords Solar radio bursts, radio communications, cell phones, space weather.

1. INTRODUCTION

In the last 150 years, the number of technologies embedded in space-affected environments has vastly increased, and continue to do so. The sophistication of the technologies and how they relate to the environments in which they are embedded means that ever more detailed understanding of both the technologies and the physical environments is needed (e.g., Lanzerotti

I.A. Daglis (ed.), Effects of Space Weather on Technology Infrastructure, 203-213.

2001). This paper summarizes research into the potential effects of solar radio emissions on some wireless technologies. This work is motivated by the evidence presented in Figure 1 (from Lanzerotti et al. 1999) for an increase in dropped call rates on one day in the hour at sunrise in the wireless system of one state of the United States that appeared to be associated with a solar radio event during that interval.

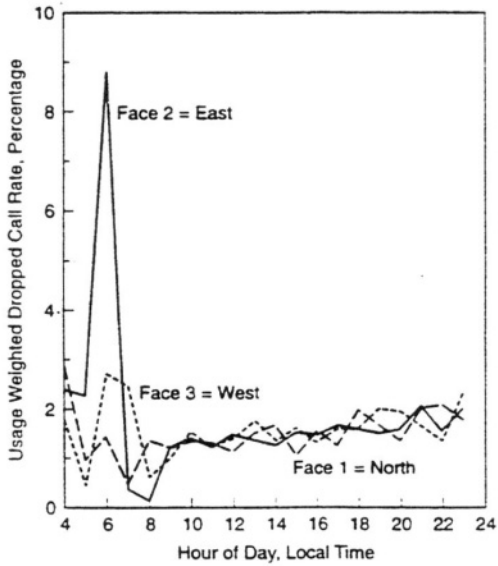

Figure 1. Usage-weighted dropped call rate for a wireless system base station, showing an enhanced level of dropped calls on the east-facing receivers near local sunrise. From Lanzerotti et al. (1999).

Microwave emissions from the sun were first reported by Southworth (1945). Radio bursts at the time of solar activity were discovered to be the source of interference in World War II radar systems (rather than by deliberate enemy jamming; Hey, 1946). Indeed, the first occurrence of this "natural" jamming was the result of intense solar activity (on 28 February 1942) that produced the first-ever measured ground level enhancement of "cosmic" rays (Forbush, 1946). Since their discovery, solar radio bursts have long been of applied-research interest for numerous reasons, including their possible predictive use for solar particle events (e.g., Castelli et al., 1973)—which in turn can cause radiation effects on spacecraft and polar-flying aircraft, and enhanced ionization in the ionosphere. Solar radio bursts continue to be of applied research interest in view of their potential interference in radar systems, satellite communication systems, and wireless.

The evidence for solar-burst influence on existing wireless systems remains indirect due to the proprietary nature of the data pertaining to system outages. Our approach, outlined in section 2, has been to examine the potential for solar bursts to affect cell-phone base stations based on our understanding of the noise and error-correction characteristics of the cell-phone waveform. We find that solar bursts exceeding about 1000 sfu (solar flux units, 1 sfu = 10^{-22} W m^{-2} Hz^{-1}) can potentially cause significant interference when the Sun is within the base-station antenna beam, which can happen for east- or west-facing antennas during sunrise and sunset at certain times of the year. In section 3 we describe the temporal and frequency characteristics of large solar bursts, using examples from the Bell Labs/NJIT Solar Radio Spectropolarimeter (SRSP) and the Owens Valley Solar Array (OVSA), operated by New Jersey Institute of Technology. We give attention to these characteristics across the entire microwave frequency band, not just the operating bands of current systems, in anticipation of future wireless systems that will undoubtedly go to higher frequencies. In section 4 we provide an overview of results of the studies we have carried out to establish the occurrence rate of solar bursts exceeding 1000 sfu. We conclude in section 5 with a discussion of the impact of solar bursts on future wireless technology.

2. SOLAR RADIO BURST FLUX THRESHOLD FOR IMPACT ON WIRELESS SYSTEMS

The discussions in Bala et al. (2002), in Nita et al. (2002) and in Lanzerotti et al. (2003) present some of the considerations of noise levels for wireless systems. For an ambient operating temperature T = 273 K, the nominal thermal noise power level P_T for a receiver of bandwidth B = 1 Hz is 3.8 x 10^{-21} W (~ −174 dBm), or 38 sfu Hz m^2. A single polarization antenna of gain G that is immersed in an isotropic radio flux of F W m^{-2} will have a receiver power of (Kummer and Gillespie, 1978)

$$P_R = G\,B\,\lambda^2 F/(8\pi) \quad \text{W Hz}^{-1} \tag{1}$$

where λ is the carrier wavelength. If F_{eq} is defined as an "equivalent" solar flux in sfu where the thermal and the solar noise levels are equal, then

$$kT\,B = G\,B\,\lambda^2 F_{eq}/(8\pi). \tag{2}$$

From (2), F_{eq} will be ~ 960 sfu for a typical cellular base station with an antenna $G \sim 10$ that is operating near 1 GHz ($\lambda^2 \sim 0.1$ m^2). Thus the total input noise $P_T + P_R$ will be more than 3 dB above thermal for $F > F_{eq}$. F_{eq} could range from ~ 1000 sfu to as low as ~ 300 sfu for an operating frequency $f \sim 1$ GHz since gains of cell site antennas can typically range from 10 to 30.

Thus, we take a flux density of ~ 10^3 sfu, the point where the noise floor rises by a factor of two, as the limit beyond which a solar radio burst can potentially affect cell-phone systems. We will investigate the likelihood of occurrence of bursts of this magnitude in Section 4, but first we give a few examples of dynamic spectra (flux density resolved in frequency and time) for large solar radio bursts to provide an overview of their characteristics.

3. SOME EXAMPLES OF SOLAR RADIO BURST DYNAMIC SPECTRA

Before discussing the occurrence rate of bursts, which merely refers to a single flux measurement at the time of maximum flux, it is worthwhile to give an overview of the spectral dynamics of typical large bursts. Some bursts show a simple, single peak in both time and frequency, for which the potential for impact on wireless systems is limited to a short duration at a small range of frequencies. However, the larger bursts typically show multiple temporal and spectral peaks, with significant complexity.

Figure 3, from the Bell Labs/NJIT SRSP radiotelescope, shows an example of a rather simple burst observed at 120 frequencies in the range 1.46-15.5 GHz, reaching a maximum flux density of about 1100 sfu near 5 GHz. Note, however, the narrow spike at the beginning of the burst, which appears in only one sample (time resolution 2 s) and reaches nearly 1300 sfu. The peak flux density may have been higher still if better time resolution were used. It is worth keeping in mind that the burst statistics we discuss in the next section were taken at a few fixed frequencies and with unexceptional time resolution, so generally the peak flux densities may be expected to be higher than the reported ones.

In Figure 4 we show a more typical large burst, observed with OVSA. Here the peak flux density exceeds 6000 sfu, and the burst displays multiple peaks in both time and frequency. In addition to the main spectral component at cm wavelengths (at frequencies $f > 3$ GHz), which is due to gyrosynchrotron radiation from electrons spiralling in the coronal magnetic field, there is also a strong and variable low-frequency component ($f < 3$ GHz) due to plasma processes in a higher coronal source. The burst remains

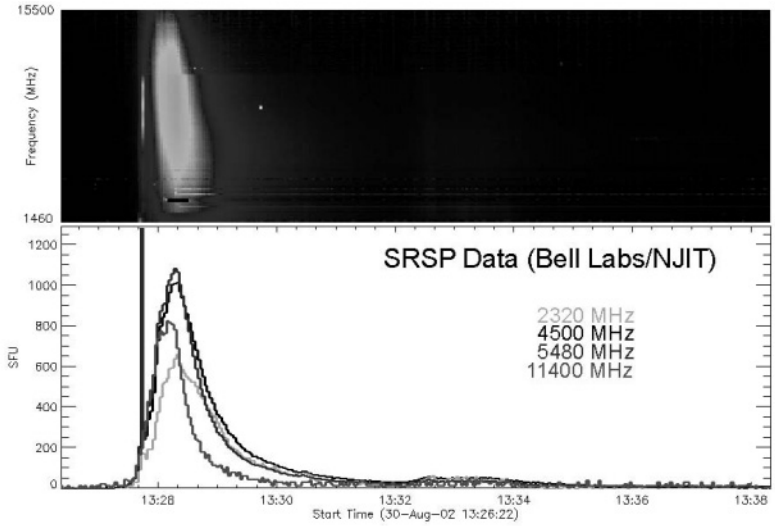

Figure 3. A simple solar burst on 2003 Aug 30, as observed with SRSP. The dynamic spectrum is shown in the upper panel, where colors represent the radio flux density, shown on a logarithmic color scale. Time is plotted horizontally, and frequency is plotted on the vertical scale, increasing upward. Time profiles at 4 representative frequencies are shown in the bottom panel.

above our 1000 sfu threshold for minutes at a time. Other bursts have been measured to remain above the threshold for as much as an hour.

4. STATISTICS OF OCCURRENCE OF SOLAR RADIO BURSTS

To establish the occurrence rate of solar bursts as a function of peak flux density and frequency, we have performed several studies whose results are summarized here. The work is described in more detail in Bala et al. (2002), Nita et al. (2002), and Nita et al. (2003). For the first two studies, we used the world-wide database of solar bursts compiled by the National Geophysical Data Center (NGDC) of the National Oceanic and Atmospheric Administration (NOAA). The database comprises 40 years of burst reports gathered from dozens of reporting stations around the world, from 1960-1999. The reports are limited to a single flux density per operating frequency for each burst, taken at the time of maximum flux density at that frequency.

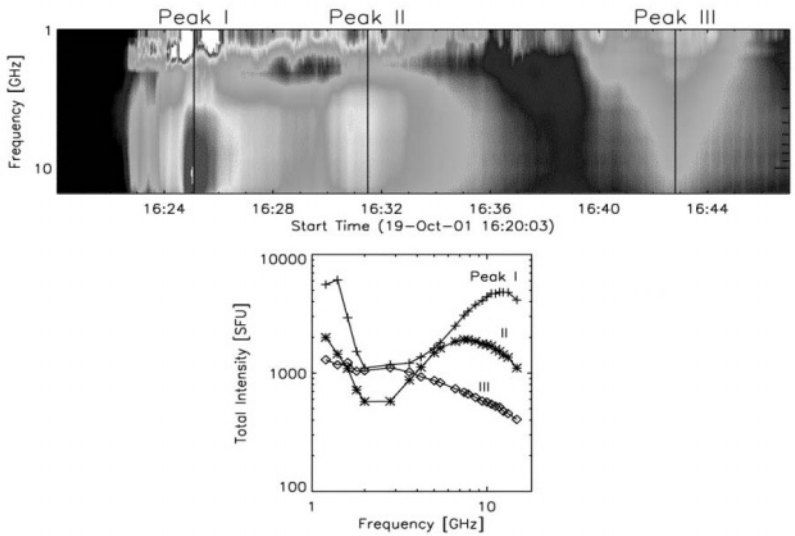

Figure 4. A large solar burst on 2001 Oct 19, as observed with OVSA. The dynamic spectrum is shown in the upper panel, as in Fig. 3, except frequency is plotted increasing downward. Vertical lines are drawn at the times of three main peaks in the emission, and the instantaneous spectra at each time are shown in the lower panel.

The dataset contains over ½ million entries concerning some 150,000 bursts. The third study consists of a database of 412 events observed over two years from 2001-2002 with OVSA. This database gives more detailed information in the form of high-resolution spectra as a function of time over the entire burst duration, as shown in Fig. 4, and was used to confirm and extend the findings from the earlier studies.

Table 1 shows some statistics of the entire NOAA dataset for all 40 years (first row), broken down by solar cycle (next three rows), and broken down by phase of the cycle (bottom two rows). The number of events per hour (last column) shows a factor of 3 increase from solar minimum to solar maximum, reaching about 0.83 events/hr. This is the observed rate of occurrence for all reported events, regardless of their flux density (down to 10-50 sfu, depending on the reporting station).

Wheatland (2000) among others has pointed out that the event occurrence rate (or its inverse, the waiting time between events) should not be determined from an average over a long period of time because the phenomenon is non-stationary—that is, the rate itself varies over time. Nita et al. (2002) did an analysis of waiting times by forming a distribution of time of occurrence of each burst relative to its predecessor, and found that the distribution of mean waiting times takes the form of an exponential. In

Year range	N_{events}	$\langle \Delta t_{events} \rangle$ (min)	N_{events}/T (events/hr)
1960-1999 (All 40 yrs)	155396	135.39	0.44
1966-1975 (Cycle 20)	39074	134.60	0.44
1976-1985 (Cycle 21)	59175	88.88	0.67
1986-1995 (Cycle 22)	45391	115.87	0.52
12 solar max years: 69-72, 79-82, 89-92	87516	72.11	0.83
12 solar min years: 66-67, 74-77, 84-87, 94-95	28261	223.30	0.27

Table 1. Statistics of events for the entire NOAA database.

this case one can deduce a characteristic waiting time using a functional form suggested by Wheatland (2000). The characteristic waiting time between bursts found by this method was about 80 minutes. This is to be compared with the overall *observed* waiting time for the entire dataset ($\langle \Delta t_{events} \rangle$ for all 40 years in Table 1) of 135 minutes, which is some 1.7 times longer.

The simplest explanation for this discrepancy is that a rather large fraction of bursts was missed. Nita et al. (2002) looked for evidence for missed bursts by plotting the distribution of occurrence time vs. time of day. Since solar bursts would not be expected to favor any particular hour of the day, any non-random distribution of time of day might be attributable to missed bursts at some geographical locations. Figure 5 shows the results of such hourly distributions. There are, indeed, significant peaks in the hourly distributions which indicate that some Earth longitudes are better covered for solar radio measurements than others. Nita et al. (2002) made the assumption that the peaks of these distributions represent the true rate (i.e., observing stations at those longitudes did not miss any events), and therefore that the ratio of filled area to total area at this peak number level represents the total number of missed events. Plots like those in Fig. 5 can thus be used to derive a "geographical correction factor," C_{geo}. It is remarkable that although it varies over time, C_{geo} was found to be close to the factor of 1.7 expected from the waiting time analysis. We note in passing that the distributions of Fig. 5 seem to show an increasing percentage of missed events at U.S. longitudes in solar cycle 22 as compared to earlier cycles.

We are now ready to show the main result of Nita et al. (2002) that pertains to solar burst impact on wireless systems. This main result is the so-called cumulative distribution of events, plotted separately for solar maximum years and solar minimum years in Figure 6. A cumulative distribution has the property that a given bin contains the cumulative number of bursts at that flux density *and higher*. The number on the vertical axis is the number of events per day. The plot on the left is for solar maximum years, and the plot of the right is for solar minimum years. The actual data are shown by the binned line, while the best power law fit is shown by the solid diagonal lines. The fit is useful for parametrizing the distribution for analytical use, and the parameters of the fit are shown in each panel. The dotted lines show the same fits, but multiplied by the relevant geographical correction factor, C_{geo}, also shown in each panel.

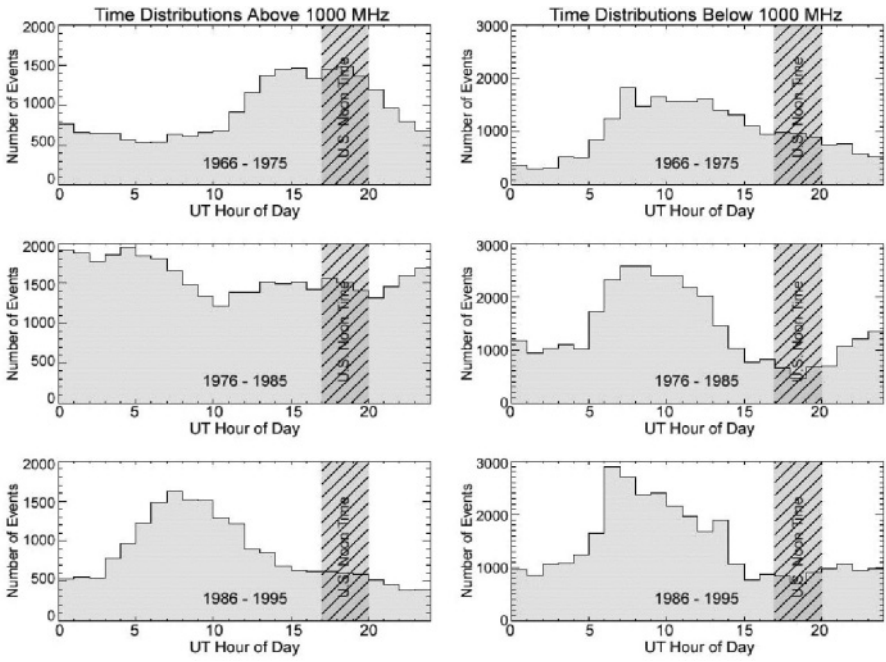

Figure 5. Plots of hourly occurrence rate of bursts in the NOAA database for events with peak frequency $f > 2$ GHz (left panels) and for events with $f < 2$ GHz (right panels). The distributions are shown separately for the three complete solar cycles 20, 21 and 22. The UT hours corresponding to noon-time time zones for the U.S. are shown as a hatched region in each plot.

As we noted in section 2, the threshold for potential impact on wireless systems is ~1000 sfu, so to determine the occurrence rate of solar bursts above this flux density at solar maximum, one merely reads the

number from the graph as shown by the arrows in the left panel of Figure 6 to get a value of about 0.28 events/day, or one event every 3.5 days, on average. To obtain this number we used the dotted line, which is the fit to the observed points corrected for missed events by multiplying by the geographical factor C_{geo}. A similar procedure (right panel) shows that the number of bursts at solar minimum falls to one event every 18.5 days.

Figure 6 shows the data and fits for all bursts above 2 GHz, meaning that bursts are counted regardless of the frequency at which they occur. Designers of current and future wireless systems may wish to evaluate potential interference only for bursts within their operating band. For this reason, Nita et al. (2002) tabulate the fit parameters $N(S > 1$ sfu) and λ, as shown in Figure 6, for burst distributions in other frequency ranges. To apply the tabulated values for a given flux density threshold S_0, one inserts the parameters into the equation

$$N(S>S_0) = N(S>1)\, S_0^{\lambda+1}.$$

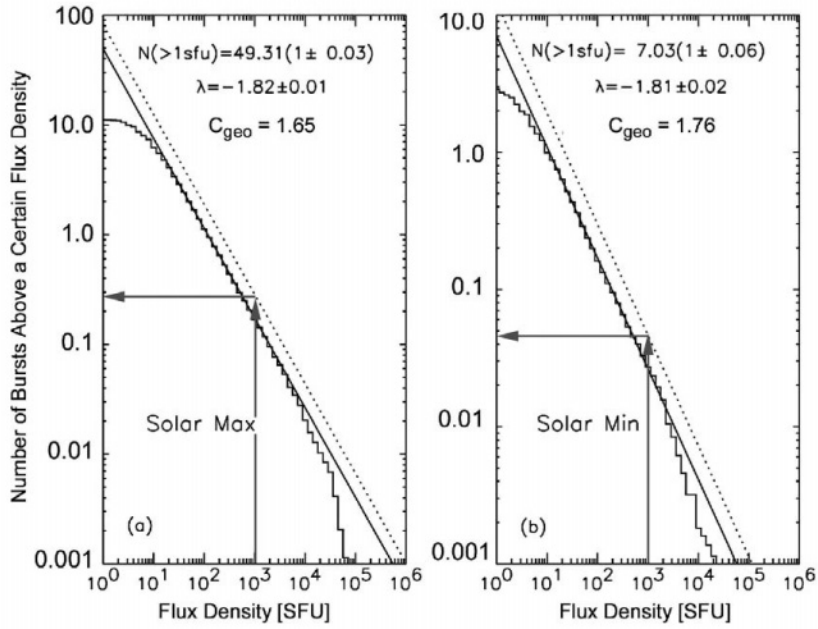

Figure 6. Cumulative distributions of number of bursts per day greater than a given flux density near solar maximum (left panel) and solar minimum (right panel). The data are shown by the histograms, and the solid lines show the best power law fit to the distributions. The fit parameters are given in the annotation. The fall of the data away from the fit at low flux densities (< 20 sfu) is due to the instrumental sensitivity limit of the reporting stations. The lack of large bursts may be a real solar effect. The dotted lines show the power law fit after multiplying by C_{geo}. The arrows show how to read the number of bursts for a given flux density threshold (10^3 sfu in this case—see text).

Recently, Nita et al. (2003) have completed another statistical study of solar bursts, this time with full temporal and spectral resolution based on two years (2001-2002) of OVSA data (see Fig. 4). Although the aim of the work was basic understanding of solar burst phenomena, some characteristics of the results are relevant to the topic of this chapter. In particular, they found that there is a relatively sharp dividing line between gyrosynchrotron bursts (above 2.6 GHz) and decimetric bursts due to coherent processes (below 2.6 GHz). The coherent bursts have flux densities that can have almost any value, so high-flux bursts are equally possible at any frequency below 2.6 GHz. Above this frequency, however, the bursts are due to gyrosynchrotron emission and show a rather clear, frequency-dependent limit of $\sim 300(f_{\mathrm{GHz}})^{2}$ sfu over the range 2.6-18 GHz. The limit is empirical, not fundamental, and appears to be due to the product of the practical limit of burst size (< 1.3 arc-minutes diameter) and the typical brightness temperature ($\sim 10^{9}$ K). Rare individual bursts can probably exceed this flux limit, but the finding offers some indication that frequencies just above 2.6 GHz are least likely to have high flux densities.

5. CONCLUSIONS

We have examined the statistical properties of solar bursts from the point of view of their potential impact on wireless systems, in particular cell-phone base stations. An analysis of the noise floor of typical base stations shows that bursts exceeding ~1000 sfu will double the noise and hence may begin to cause problems for the system if the horizon-looking antennas are pointed at the rising or setting Sun. Our analysis shows that such bursts occur on average once every 3.5 days during solar maximum and once every 18.5 days at solar minimum.

Since a given base station of a wireless system is at risk for only a short period (about 1 hour) around sunrise and sunset, a typical station may be affected at roughly $1/12^{\mathrm{th}}$ of this rate, or once per 42 days at solar maximum and once per 222 days at solar minimum. Thus, the impact may be deemed small. However, any optimism should be tempered by the facts that (1) a large geographical area will see the rising or setting Sun simultaneously, and so any impacts may be felt system-wide and (2) systems spanning multiple time zones are at risk for correspondingly longer times. Note also that the largest bursts may attain peak flux densities 10-100 times the limit of 1000 sfu that we identified as having a potential impact, so on rare occasions the impact may be more severe.

As technological systems continue to proliferate, it is wise to keep all potential environmental influences in mind. Solar radio bursts represent one aspect of Space Weather that can easily be overlooked, but may nevertheless cause problems for certain technologies. We can look forward to wireless systems moving to higher frequencies in the future. Our work indicates that wireless system operating frequencies just above 2.6 GHz are the most favorable for avoiding impacts from solar bursts, but the impacts below 2.6 GHz and above about 10 GHz are significantly higher.

6. ACKNOWLEDGEMENTS

This work was supported through an NSF Space Weather program grant ATM-0077273 to New Jersey Institute of Technology. The Owens Valley Solar Array is supported by NSF grant AST-0307670 and NASA grant NAG5-11875 to New Jersey Institute of Technology.

7. REFERENCES

Bala, B., Lanzerotti, L. J., Gary, D. E. & Thomson, D. J., Noise in wireless systems produced by solar radio bursts, Radio Science, 37(2), 10.1029/2001RS002488, 2002.

Castelli, J. P., J. Aarons, D.A. Guidice and R.M. Straka, The Solar Radio Patrol Network of the USAF and Its Application. Proc. IEEE, 61, 1307, 1973.

Forbush, S. E., Three recent cosmic-ray increases possibly due to charged particles from the Sun, Phys. Rev., 70, 771, 1946.

Hey, J. S., Solar Radiations in the 4--6 metre Radio Wavelength band, Nature, 158, 234, 1946.

Lanzerotti, L. J., Thomson, D. J., & Maclennan, C. G., Modern Radio Science, Oxford, 25, 1999.

Lanzerotti, L. J., Space Weather Effects on Communications, Space Storms and Space Weather Hazards, Proc. NATO Advanced Study Institute on Space Storms and Space Weather Hazards, (ed: I.A. Daglis), Kluwer Academic Publishers, 313, 2001.

Lanzerotti, L. J., Gary, D. E., Nita, G. M., Thomson, D. J. & Maclennan, C. G., Noise in wireless systems from solar radio bursts, Advances in Space Research, in press, 2003.

Nita, G. M., Gary, D. E., Lanzerotti, L. J. & Thomson, D. J., The Peak Flux Distribution of Solar Radio Bursts, Astrophysical Journal, 570, 2002

Nita, G. M., Gary, D. E. & Lee, J., Statistical study of two years of solar flare radio spectra obtained with OVSA, Astrophysical Journal, in press, 2003

Southworth, G.C., Microwave Radiation from the Sun, J. Franklin Inst., 239, 285, 1945.

Wheatland, M. S., The Origin of the Solar Flare Waiting-Time Distribution, Astrophysical Journal, 536, L109, 2000.